Protein Science (2000), *9*:1304–1311. Cambridge University Press. Printed in the USA.

Optimization of the catalytic properties of *Aspergillus fumigatus* phytase based on the three-dimensional structure

ANDREA TOMSCHY, MICHEL TESSIER, MARKUS WYSS, ROLAND BRUGGER, CLEMENS BROGER, LINE SCHNOEBELEN, ADOLPHUS P.G.M. VAN LOON, AND LUIS PASAMONTES

F. Hoffmann-La Roche Ltd, CH-4070 Basel, Switzerland

(RECEIVED March 7, 2000; FINAL REVISION April 12, 2000; ACCEPTED April 28, 2000)

Abstract

Previously, we determined the DNA and amino acid sequences as well as biochemical and biophysical properties of a series of fungal phytases. The amino acid sequences displayed 49–68% identity between species, and the catalytic properties differed widely in terms of specific activity, substrate specificity, and pH optima. With the ultimate goal to combine the most favorable properties of all phytases in a single protein, we attempted, in the present investigation, to increase the specific activity of *Aspergillus fumigatus* phytase. The crystal structure of *Aspergillus niger* NRRL 3135 phytase known at 2.5 Å resolution served to specify all active site residues. A multiple amino acid sequence alignment was then used to identify nonconserved active site residues that might correlate with a given favorable property of interest. Using this approach, Gln27 of *A. fumigatus* phytase (amino acid numbering according to *A. niger* phytase) was identified as likely to be involved in substrate binding and/or release and, possibly, to be responsible for the considerably lower specific activity (26.5 vs. 196 $U \cdot [mg\ protein]^{-1}$ at pH 5.0) of *A. fumigatus* phytase when compared to *Aspergillus terreus* phytase, which has a Leu at the equivalent position. Site-directed mutagenesis of Gln27 of *A. fumigatus* phytase to Leu in fact increased the specific activity to 92.1 $U \cdot (mg\ protein)^{-1}$, and this and other mutations at position 27 yielded an interesting array of pH activity profiles and substrate specificities. Analysis of computer models of enzyme–substrate complexes suggested that Gln27 of wild-type *A. fumigatus* phytase forms a hydrogen bond with the 6-phosphate group of *myo*-inositol hexakisphosphate, which is weakened or lost with the amino acid substitutions tested. If this hydrogen bond were indeed responsible for the differences in specific activity, this would suggest product release as the rate-limiting step of the *A. fumigatus* wild-type phytase reaction.

Keywords: 3D structure; active site; homology modeling; phytase; site-directed mutagenesis

Phytases (*myo*-inositol hexakisphosphate 3- or 6-phosphohydrolases; EC 3.1.3.8 and 3.1.3.26) belong to the family of histidine acid phosphatases (van Etten, 1982; Pasamontes et al., 1997a) and are mainly found in plants, fungi, and other microorganisms. Phytases hydrolyse phytate (*myo*-inositol hexakisphosphate)—the major storage form of phosphorus in plants—to lower *myo*-inositol phosphates and inorganic phosphate (for a review, see Wodzinski & Ullah, 1996). Because monogastric animals like pigs and poultry virtually lack phytase activity in the digestive tract, phytic acid phosphorus bioavailability from feed ingredients of plant origin is low. This necessitates supplementation of the feed with either inorganic phosphate or with phytase. Supplementation with phytase is preferable because it reduces environmental phosphorus pollution by animal manure (for a review, see Wodzinski & Ullah, 1996). Phytic acid is also regarded as an antinutritional factor because of its strong chelating properties—complexing metal ions and proteins and thereby decreasing their absorption in the gastrointestinal tract—which can as well be relieved by supplementation of the feed with phytase.

We have isolated and characterized the genes for different fungal phytases (Mitchell et al., 1997; Pasamontes et al., 1997a, 1997b) and have overexpressed the proteins in yeasts or filamentous fungi. Biochemical characterization of these phytases (Wyss et al., 1998, 1999a, 1999b) revealed a wide variety of biochemical and biophysical properties with regard to protein stability, substrate specificity, and pH dependence of activity. *Aspergillus fumigatus* phytase showed a series of favorable properties, such as broad substrate specificity, a broad pH optimum, efficient refolding after heat denaturation (Pasamontes et al., 1997b; Wyss et al., 1998), and superior performance in animal trials than *Aspergillus niger* phytase in terms of increasing phosphorus digestibility (Simões Nunes & Guggenbuhl, 1998). However, it displayed a relatively low specific

Reprint requests to: Luis Pasamontes, Roche Vitamins Inc., Bldg. 102, 340 Kingsland Street, Nutley, New Jersey 07110-1199; e-mail: luis.pasamontes@roche.com

activity at pH 5.0 of 26.5 U·(mg protein)$^{-1}$ compared to 102.5 U·(mg protein)$^{-1}$ for *A. niger* phytase or 196 U·(mg protein)$^{-1}$ for *Aspergillus terreus* CBS phytase (Wyss et al., 1999a). The specific activity is, however, a key factor for commercial exploitation because it has an impact on the economy of the intended use. Our aim, therefore, was to improve the enzymatic properties of *A. fumigatus* phytase on the basis of the three-dimensional (3D) structure of *A. niger* NRRL 3135 phytase (Kostrewa et al., 1997).

Results

Comparison of the catalytic properties of the parent wild-type phytases

A. fumigatus ATCC 13073 and *A. terreus* CBS phytase display distinct differences in enzymatic properties (Wyss et al., 1999a). While the specific activity of *A. fumigatus* phytase is rather low, 26.5 U·(mg protein)$^{-1}$ at pH 5.0, it is relatively unaffected by pH, with >80% of the maximal specific activity between pH 4.0 and 7.3. In addition, *A. fumigatus* phytase has broad substrate specificity, displaying considerable hydrolytic activity with a range of structurally diverse phosphate compounds. On the other hand, *A. terreus* CBS phytase displays high specific activity at its pH optimum of 5.5, around 200 U·(mg protein)$^{-1}$, but its pH optimum and substrate specificity are more narrow than those of *A. fumigatus* phytase. Our goal was to increase the specific activity of *A. fumigatus* phytase on the basis of its modeled 3D structure, while maintaining broad substrate specificity and high activity over a broad pH range.

Identification of active site residues

Based on the 3D structure of *A. niger* NRRL 3135 phytase (Kostrewa et al., 1997), 43 residues pointing into the active site cavity were identified (Fig. 1). Comparison of the amino acid sequences of *A. fumigatus*, *A. niger*, and *A. terreus* phytase showed that 24 of these positions are identical among these three phytases. All these residues are also conserved in *Emericella nidulans* and *A. terreus* 9A1 phytase, while most are conserved in *Talaromyces thermophilus* (except D202 and T209) and *Myceliophthora thermophila* phytase (except S67, K68, T209, and L273; Mitchell et al., 1997; Pasamontes et al., 1997a). All highly conserved active site residues except K278 are located on one side of the active site cavity, around the catalytically active His59, and all nonconserved residues on the opposite side. Among the nonconserved active site residues that might have correlated with the high specific activity of *A. terreus* phytase, residue No. 27 was seen to have a major effect on the catalytic properties.

Amino acid substitutions at position 27 affect the pH-dependence of catalytic activity

Nine different substitutions were made at position 27 of *A. fumigatus* phytase, with some of them drastically increasing specific activity (Fig. 2). The specific activities at the respective pH optima ranged from 21 (*A. fumigatus* Q27P phytase) to 238 U·(mg protein)$^{-1}$ (*A. fumigatus* Q27I phytase). At pH 5.0, the specific activities ranged from 15.5 (*A. fumigatus* Q27P phytase) to 92.1 U·(mg protein)$^{-1}$ (*A. fumigatus* Q27L phytase; see Table 1). The pH-activity profiles of the various phytases differed significantly from each other. *A. fumigatus* wild-type phytase showed more or less constant specific activity over a broad pH range. The pH-activity profile of the Q27A mutant resembled that of *A. fumigatus* wild-type phytase with slight increases below pH 4.0 and around pH 6.5. The Q27G and Q27N mutants showed increases in specific activity that were almost constant over the entire pH range. The amino acid substitutions Q27L and Q27I resulted in a remarkable increase in specific activity around pH 6.5, while having no or only a modest effect in the more acidic pH range. Interestingly, the shape of the pH-activity profiles of the Q27L and Q27I mutants strongly resembles that of *A. terreus* CBS phytase—which also has a leucine at position 27—although the pH optimum is shifted by 1 unit toward neutrality (6.5 vs. 5.5). The Q27T mutant showed an interesting pH-activity profile that "combined" the favorable effects of the Q27I and Q27L mutants on one hand (increase in specific activity around pH 6.5) and of the Q27G and Q27N mutants on the other hand (increase in specific activity over the entire pH range). Compared to wild-type *A. fumigatus* phytase, it revealed an approximately two- to threefold increase in specific activity also at low pH values (pH 3.0–5.0), combined with a peak value of about 130 U·(mg protein)$^{-1}$ at pH 6.5. The Q27P mutant showed a pronounced tendency to aggregate and precipitate; therefore, the results obtained with this mutant have to be interpreted with caution. Finally, the "inverse" mutation, L27Q, in *A. terreus* CBS phytase strongly decreased the specific activity, from 195.8 to 35.4 U·(mg protein)$^{-1}$ (Table 1). All these results demonstrate that residue 27 plays a key role in determining the specific activity of *A. fumigatus* and *A. terreus* phytase.

Mutations at position 27 of A. fumigatus phytase have little effect on substrate specificity, but may affect thermostability

The different mutant phytases were tested for their specific activities with a wide range of phosphorylated substances (Fig. 3). When compared to the profound differences in substrate specificity between individual fungal wild-type phytases (Wyss et al., 1999a), the impact of the amino acid substitutions at position 27 of *A. fumigatus* phytase was relatively minor. Some of the mutants

Table 1. *Specific activity of A. fumigatus and A. terreus CBS wild-type and mutant phytases under standard assay conditions at pH 5.0*

	Specific activity [U/mg]	*n*
A. fumigatus wild-type phytase	26.5 ± 5.2[a]	22
A. fumigatus Q27N	45.6 ± 2.5	4
A. fumigatus Q27T	75.2 ± 11.4	8
A. fumigatus Q27L	92.1 ± 6.5	6
A. fumigatus Q27I	82.3 ± 7.8	3
A. fumigatus Q27V	33.9 ± 2.1	4
A. fumigatus Q27A	29.4 ± 5.5	3
A. fumigatus Q27G	61.7 ± 5.9	5
A. fumigatus Q27S	51.1 ± 10.1	4
A. fumigatus Q27P	15.5 ± 1.8	4
A. terreus CBS wild-type phytase	195.8 ± 17.8[a]	7
A. terreus CBS L27Q	35.4 ± 6.0	4

[a] Data from Wyss et al. (1999a).

```
                                    #Δ#
Anig ASRNQSSCDTVDQGYQCFSETSHLWGQYAPFFSLANESVISPEVPAGCRV 50
Afum ....SKSCDTVDLGYQCSPATSHLWGQYSPFFSLEDELSVSSKLPKDCRI 46
Ater .....SDCTSVDRGYQCFPELSHKWGLYAPYFSLQDESPFPLDVPDDCHI 45

            ### #  #Δ##  Δ#
Anig TFAQVLSRHGARYPTDSKGKKYSALIEEIQQNATTFDGKYAFLKTYNYSL 100
Afum TLVQVLSRHGARYPTSSKSKKYKKLVTAIQANATDFKGKFAFLKTYNYTL 96
Ater TFVQVLARHGARSPTDSKTKAYAATIAAIQKNATALPGKYAFLKSYNYSM 95

       Δ                                        Δ #
Anig GADDLTPFGEQELVNSGIKFYQRYESLTRNIVPFIRSSGSSRVIASGKKF 150
Afum GADDLTPFGEQQLVNSGIKFYQRYKALARSVVPFIRASGSDRVIASGEKF 146
Ater GSENLTPFGRNQLQDLGAQFYRRYDTLTRHINPFVRAADSSRVHESAEKF 145

                                       #        Δ Δ    ##  Δ
Anig IEGFQSTKLKDPRAQPGQSSPKIDVVISEASSSNNTLDPGTCTVFEDSEL 200
Afum IEGFQQAKLADPGA.TNRAAPAISVIIPESETFNNTLDHGVCTKFEASQL 195
Ater VEGFQNARQGDPHANPHQPSPRVDVVIPEGTAYNNTLEHSICTAFEASTV 195

      #  Δ   #                            Δ  ΔΔ  Δ   #
Anig ADTVEANFTATFVPSIRQRLENDLSGVTLTDTEVTYLMDMCSFDTISTST 250
Afum GDEVAANFTALFAPDIRARAEKHLPGVTLTDEDVVSLMDMCSFDTVARTS 245
Ater GDAAADNFTAVFAPAIAKRLEADLPGVQLSADDVVNLMAMCPFETVSLTD 245

                          #Δ #Δ  Δ#  #Δ
Anig VDTKLSPFCDLFTHDEWINYDYLQSLKKYYGHGAGNPLGPTQGVGYANEL 300
Afum DASQLSPFCQLFTHNEWKKYNYLQSLGKYYGYGAGNPLGPAQGIGFTNEL 295
Ater DAHTLSPFCDLFTAAEWTQYNYLLSLDKYYGYGGGNPLGPVQGVGWANEL 295

                                          ##Δ
Anig IARLTHSPVHDDTSSNHTLDSSPATFPLKSTLYADFSHDNGIISILFALG 350
Afum IARLTRSPVQDHTSTNSTLVSNPATFPLNATMYVDFSHDNSMVSIFFALG 345
Ater IARLTRSPVHDHTCVNNTLDANPATFPLNATLYADFSHDSNLVSIFWALG 345

                                  Δ     #
Anig LYNGTKPLSTTTVENITQTDGFSSAWTVPFASRLYVEMMQCQAEQAPLVR 400
Afum LYNGTEPLSRTSVESAKELDGYSASWVVPFGARAYFETMQCKSEKEPLVR 395
Ater LYNGTKPLSQTTVEDITRTDGYAAAWTVPFAARAYIEMMQCRAEKQPLVR 395


Anig VLVNDRVVPLHGCPVDALGRCTRDSFVRGLSFARSGGDWAECFA 444
Afum ALINDRVVPLHGCDVDKLGRCKLNDFVKGLSWARSGGNWGECFS 439
Ater VLVNDRVMPLHGCAVDNLGRCKRDDFVEGLSFARAGGNWAECF. 438
```

Fig. 1. Primary sequence alignment of *A. niger* NRRL 3135, *A. fumigatus* ATCC 13073, and *A. terreus* CBS 116.46 phytase. (#) Identical residues and (△) nonidentical residues of which the side chains are exposed to the active site cavity. All numberings used in the paper correspond to the amino acid numbering of mature *A. niger* phytase (Wyss et al., 1999b).

showed significantly higher specific activities than other mutants with selected substrates, for example, the Q27G mutant with phosphoenolpyruvate. Interestingly, although *A. terreus* CBS phytase—having leucine at the corresponding position—displays narrow substrate specificity (Wyss et al., 1999a), this latter characteristic, in contrast to the pH-dependent increase in specific activity with phytic acid (Fig. 2), was not transferred to *A. fumigatus* phytase by the Q27L mutation.

For differential scanning calorimetry experiments, where larger quantities of purified enzyme were required, some proteins were expressed in the methylotrophic yeast *Hansenula polymorpha* (see Wyss et al., 1999b). The *A. fumigatus* and *A. terreus* CBS wild-type phytases displayed unfolding temperatures T_m of 62.5 and 58.5 °C, respectively. While the T_m of the *A. fumigatus* Q27L mutant was decreased to 56.0 °C, the T_m of the Q27T mutant was identical to that of the *A. fumigatus* wild-type enzyme. No explanation at the molecular level is yet available for the peculiar, destabilizing effect of the Q27L mutation.

All A. fumigatus phytase mutants degrade phytic acid to myo-inositol monophosphate

Phytic acid degradation kinetics at pH 5.0 were investigated for mutants Q27T, Q27L, Q27I, Q27G, and Q27A, as well as for

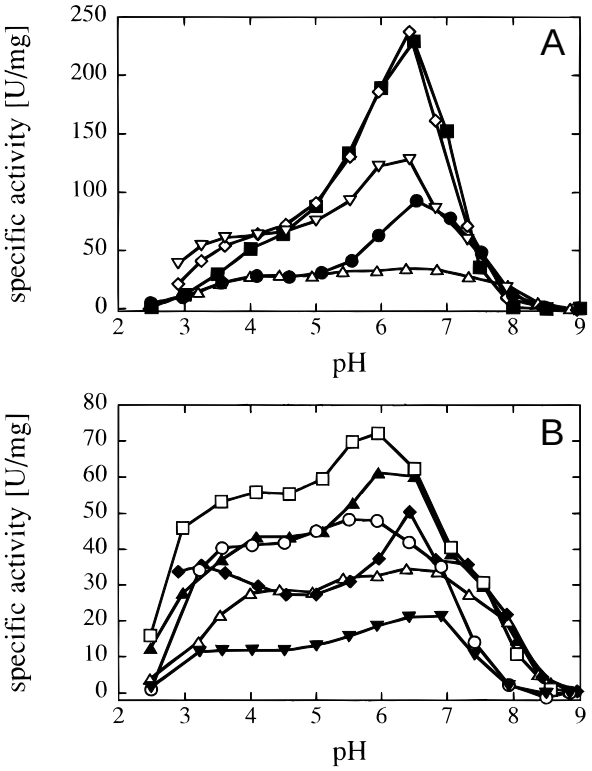

Fig. 2. pH-Activity profiles of wild-type *A. fumigatus* phytase and 9 single-site mutants. **A:** △, *A. fumigatus* wild-type phytase; ■, *A. fumigatus* Q27L phytase; ◇, *A. fumigatus* Q27I phytase; ▽, *A. fumigatus* Q27T phytase; ●, *A. fumigatus* Q27V phytase. **B:** △, *A. fumigatus* wild-type phytase; ▲, *A. fumigatus* Q27N phytase; □, *A. fumigatus* Q27G phytase; ◆, *A. fumigatus* Q27A phytase; ○, *A. fumigatus* Q27S phytase; ▼, *A. fumigatus* Q27P phytase.

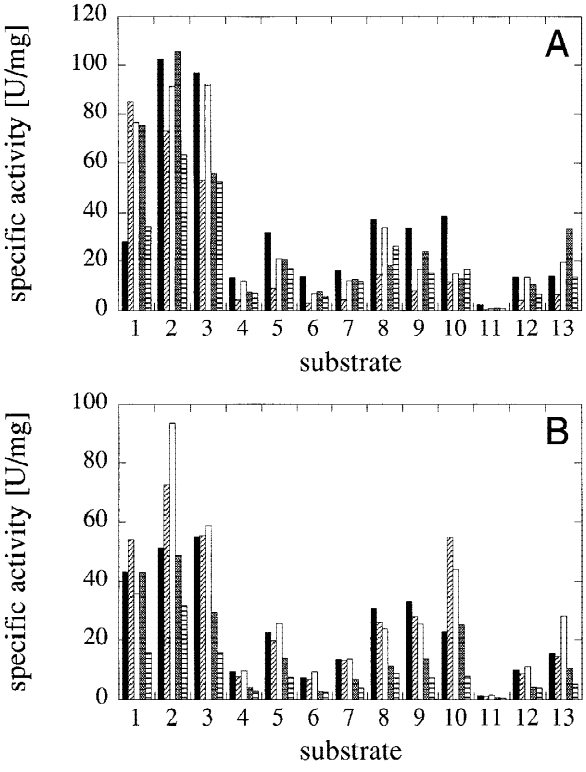

Fig. 3. Substrate specificity of wild-type and mutant *A. fumigatus* phytases. The following substrates were used at 5 mM concentrations as described under Materials and methods: (1) phytic acid; (2) *p*-nitrophenyl phosphate; (3) fructose-1,6-bisphosphate; (4) fructose-6-phosphate; (5) glucose-6-phosphate; (6) ribose-5-phosphate; (7) α-glycerophosphate; (8) β-glycerophosphate; (9) 3-phosphoglycerate; (10) phosphoenolpyruvate; (11) AMP; (12) ADP; (13) ATP. The specific activities of the different phytases (at pH 5.0) with any one of the 13 substrates tested are shown in the following order (from left to right): (**A**) *A. fumigatus* wild-type phytase and the Q27L, Q27I, Q27T, and Q27V mutants; (**B**) *A. fumigatus* Q27N, Q27G, Q27A, Q27S, and Q27P mutants.

A. fumigatus wild-type phytase. Tritium-labeled *myo*-inositol hexakisphosphate (0.2 mM) was used as substrate, and the accumulating intermediates were quantified after high-performance liquid chromatography (HPLC) separation (Fig. 4). At a protein concentration of 0.25 μg/mL, the Q27T and Q27I mutants were most efficient, causing rapid disappearance of the hexakisphosphate and considerable accumulation, after 90 min, of both the bis- and monophosphates. *A. fumigatus* wild-type phytase was least efficient on a mg/mL basis. Two further findings are worth mentioning. (1) Compared to the other enzymes analyzed, the Q27L mutant showed more pronounced accumulation of the *myo*-inositol tetrakisphosphate and very slow hydrolysis of the trisphosphate intermediate. This suggests that the Q27L mutation either decreases the specific activity with lower inositol phosphates or increases the susceptibility of the enzyme to product inhibition. (2) The Q27A mutant, although showing an almost identical *initial* rate of phosphate release from *myo*-inositol hexakisphosphate as the wild-type enzyme (compare Figs. 4A and 4F), was more efficient in further degradation of the intermediates, suggesting that this mutation selectively increases the specific activity with lower *myo*-inositol phosphates. In experiments at higher enzyme concentration, all mutants—similar to all fungal wild-type phytases analyzed so far (Wyss et al., 1999a)—degraded phytic acid completely to *myo*-inositol monophosphate, with the Q27L mutant again being least efficient in degrading the lower *myo*-inositol phosphate intermediates (data not shown).

In a complementary experiment, the time course of phosphate liberation was monitored at pH 4.0, 5.0, and 6.0, at a fixed enzyme concentration of 0.25 μg/mL and a limiting substrate concentration of 0.2 mM (Fig. 5). Complete degradation of *myo*-inositol hexakisphosphate to *myo*-inositol monophosphate should liberate 1.0 mM of inorganic phosphate, provided that the commercial preparation were 100% pure. Under the tested experimental conditions, a maximal free inorganic phosphate concentration of about 0.81–0.83 mM was reached by mutants Q27T, Q27I, and Q27N at pH 5.0. The highest initial rate of phosphate liberation was observed for mutants Q27T and Q27I, followed by Q27L, Q27N, and the other single mutants tested. Mutant Q27L, despite a high initial rate, showed considerably slower phosphate liberation beyond 30 min of incubation. After 90 min, inorganic phosphate liberation by the Q27L mutant reached 0.72 mM, which was lower than for all other mutants tested.

At pH 6.0, all mutants reached near-maximum values of liberated phosphate within 30 min of incubation, while *A. fumigatus* wild-type phytase required 50 min. The concentration of liberated phosphate increased only marginally with longer incubation times. Maximal values after 90 min ranged between 0.51 and 0.62 mM.

At pH 4.0, the profiles of the phytase variants differed widely. For all enzymes tested, the initial rate of phosphate liberation was

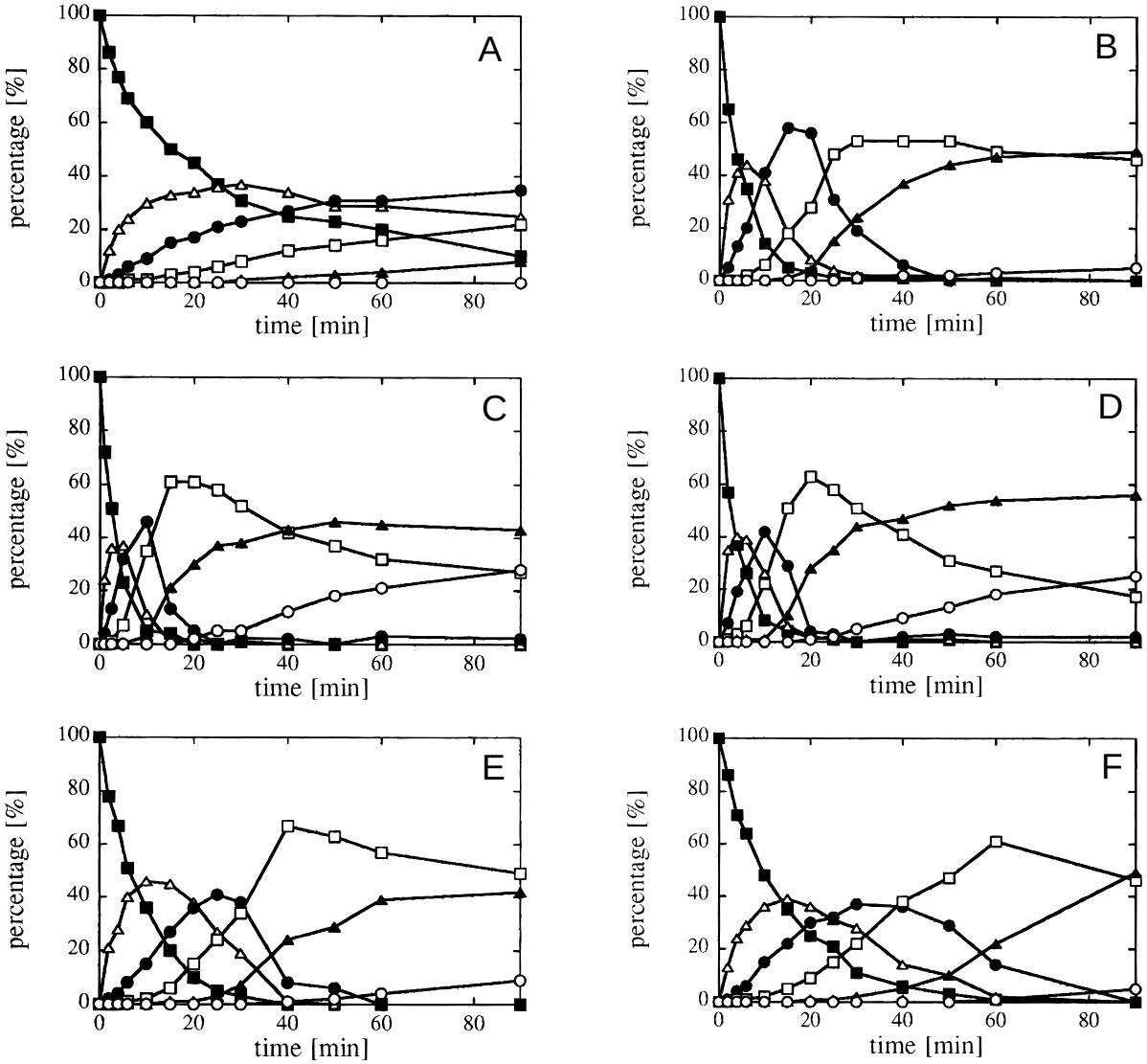

Fig. 4. Time course of phytic acid degradation and accumulation of *myo*-inositol phosphate intermediates. ■, *Myo*-inositol hexakisphosphate; △, *myo*-inositol pentakisphosphate; ●, *myo*-inositol tetrakisphosphate; □, *myo*-inositol trisphosphate; ▲, *myo*-inositol bisphosphate; ○, *myo*-inositol monophosphate. *A. fumigatus* (**A**) wild-type phytase and the (**B**) Q27L, (**C**) Q27I, (**D**) Q27T, (**E**) Q27G, and (**F**) Q27A mutants were tested at a concentration of 0.25 μg/mL.

lower than at pH 5.0 or 6.0. Mutants Q27N and Q27G, and to a lesser extent also Q27L and Q27T, showed an acceleration of phosphate liberation at intermediate stages of phytic acid degradation (Q27T after 15 min, Q27N, Q27G, and Q27L after 30 min). Such an acceleration was not observed for the other phytases investigated, although more complete phytic acid degradation would be required for the *A. fumigatus* wild-type enzyme and the Q27V and Q27A mutants to confirm the latter statement. The concentrations of inorganic phosphate after 90 min of incubation varied between 0.23 mM (wild-type phytase) and 0.69 mM (mutant Q27N).

It is evident that the data shown in Figures 4 and 5 do not fully conform with the specific activities and pH-activity profiles shown in Figure 2. This is not surprising, because the former experiments were performed at a substrate concentration of 0.2 mM and achieved almost complete degradation of phytic acid, while the latter were done as initial rate measurements at 5 mM phytic acid concentration. Therefore, the qualitative and quantitative deviations may be due to differences in K_m values and/or (product) inhibition constants.

In conclusion, the results presented in Figures 4 and 5 show (1) that the cleavage of individual phosphoester bonds in the stepwise degradation of phytic acid to *myo*-inositol monophosphate is differently affected by mutations at residue 27, and (2) that a high specific activity at saturating substrate concentrations does not necessarily reflect a high potency for complete degradation of phytic acid to *myo*-inositol monophosphate.

Discussion

The considerable sequence identity between *A. niger* and *A. fumigatus* (67%; Pasamontes et al., 1997b) or *A. terreus* CBS phytase (64%; van Loon et al., 2000) strongly suggested similar 3D structures. Using the coordinates of the crystal structure of *A. niger*

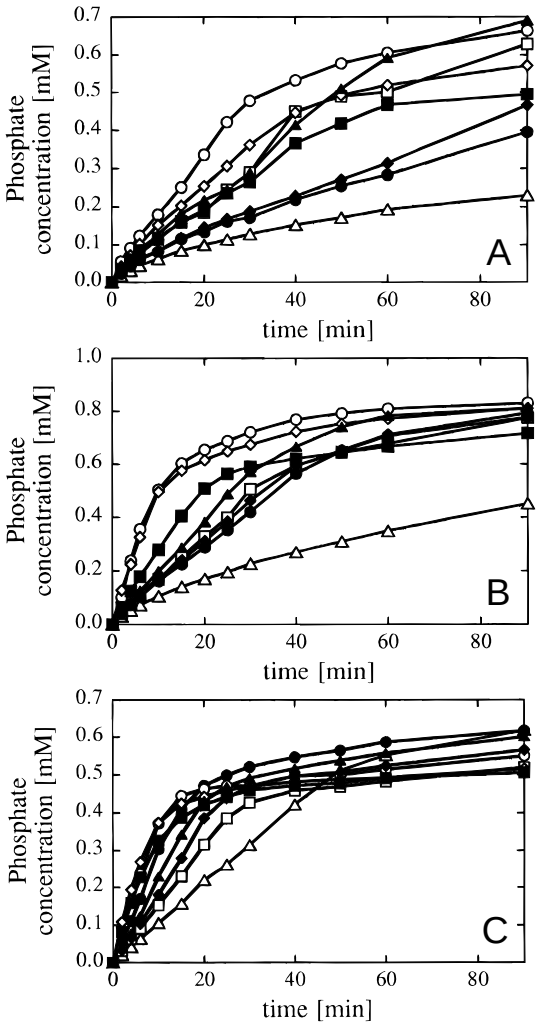

Fig. 5. Time course of phosphate liberation at (**A**) pH 4.0, (**B**) 5.0, and (**C**) 6.0 by *A. fumigatus* wild-type and mutant phytases using phytic acid as substrate. △, *A. fumigatus* wild-type phytase; □, *A. fumigatus* Q27G phytase; ▲, *A. fumigatus* Q27N phytase; ●, *A. fumigatus* Q27V phytase; ♦, *A. fumigatus* Q27A phytase; ◇, *A. fumigatus* Q27I phytase; ○, *A. fumigatus* Q27T phytase; ■, *A. fumigatus* Q27L phytase.

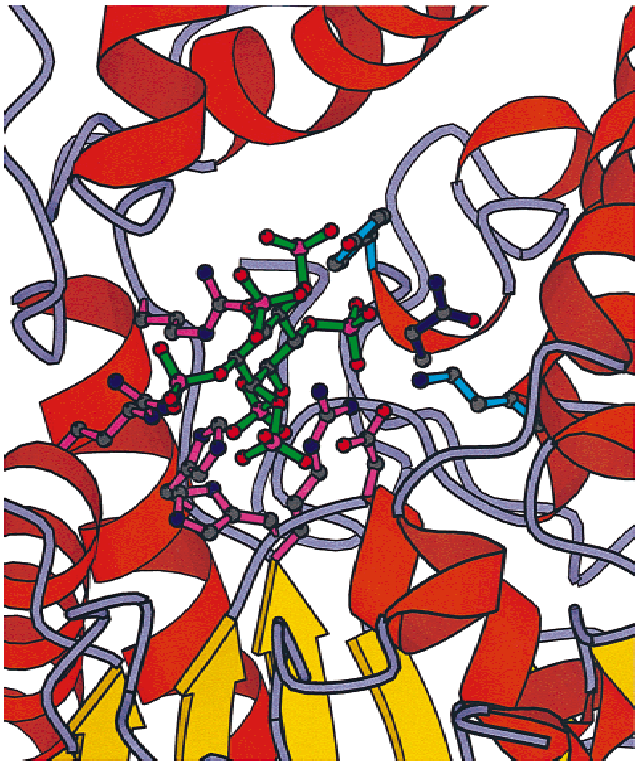

Fig. 6. Schematic view of the active site of *A. fumigatus* phytase with the substrate, phytic acid, in its hypothetical binding mode. Phytic acid is shown in green. Asp339, Arg58, His338, His59, Arg142, and Arg62 (from the lower right to the upper left on the bottom and left sides of the active site), which are fully conserved in a number of fungal phytases and fungal acid phosphatases, are represented in pink color. Tyr28 and Lys278, which are conserved in fungal phytases, are shown in light blue, and Gln27, the target residue in the present study, is shown in dark blue. For further details see Discussion.

NRRL 3135 phytase (Kostrewa et al., 1997), model structures for *A. fumigatus* and *A. terreus* CBS phytase were built by homology modeling. Only small differences between the modeled structures and the original crystal structure emerged in external loops (data not shown). Part of the active site of *A. fumigatus* phytase surrounding position 27 (numbering according to the *A. niger* phytase amino acid sequence) is shown in Figure 6.

Residues R58, R62, R142, H338, and D339 surrounding the essential H59 are conserved in all known fungal phytases (from *A. fumigatus*, *A. niger*, *A. terreus*, *E. nidulans*, *T. thermophilus*, *M. thermophila*, *Thermomyces lanuginosus*, *Trametes pubescens*, *Peniophora lycii*, *Agrocybe pediades*, *Paxillus involutus*, and *Schwanniomyces occidentalis*) and in many fungal acid phosphatases (from *A. niger*, *Pichia pastoris*, *Sacchromyces cerevisiae*, *Schizosaccharomyces pombe*, *Kluyveromyces lactis*, and *Kluyveromyces drosophilarum*; see DDBJ/EMBL/GenBank and Swiss-Prot databases). According to Kostrewa et al. (1997), the above-mentioned set of residues may be involved in phosphoester hydrolysis. The fungal phytases share additional amino acid residues within this part of the active site, namely K278 and Y28, which are not conserved in the other acid phosphatases.

The N-terminal part of *A. niger* NRRL 3135 phytase (Kostrewa et al., 1997; and most probably of all fungal phytases), consisting of about 50 amino acids, is located on the surface of the molecule. No corresponding stretch is found in the 3D structure of rat acid phosphatase (Kostrewa et al., 1997), which is largely superimposable with the *A. niger* phytase structure. The amino acids at positions 27 and 28 of phytase form a cap closing the back side of the active site. Again, no such cap is found in rat acid phosphatase.

Mutational analysis showed that changes at position 27 have profound effects on the pH-activity profile of *A. fumigatus* phytase. By replacing the glutamine present at this position in wild-type *A. fumigatus* phytase (maximal specific activity 34 U·[mg protein]$^{-1}$) by leucine as found in *A. terreus* phytase (maximal specific activity 205 U·[mg protein]$^{-1}$), a strong increase in maximal specific activity to 230 U·(mg protein)$^{-1}$ was obtained for the *A. fumigatus* Q27L mutant. A similar increase was observed for the Q27I mutant. Substitution of Q27 by the other aliphatic amino acids, alanine or valine, also caused an increase in specific activity around pH 6.5, but to a (much) lesser extent. Replacement of glutamine by glycine or asparagine did not change the shape of the

pH-activity profile, but increased the specific activity by almost a constant factor over the entire pH range of 2.5–7.5. The Q27T mutant yielded the most favorable pH-activity profile, with high specific activity over a wide range of acidic pH values.

Detailed inspection of the homology-modeled 3D structure provided a plausible explanation for the effects observed. The side chain of the nonconserved residue 27 is close to the catalytically essential residues (Fig. 6) and, therefore, also in close contact with the substrate during catalysis. Energy calculations using the program Moloc revealed that Q27 and the 6-phosphate group of *myo*-inositol hexakisphosphate bound in the hypothetical binding mode (Kostrewa et al., 1997; Lim et al., 2000) may form a hydrogen bond, while this is not possible with a Leu at this position. If the presumed hydrogen bond between Q27 and phytic acid were indeed responsible for the lower specific activity of *A. fumigatus* wild-type phytase compared to most of its mutants, this might indicate that product release is the rate-limiting step in the catalytic cycle of *A. fumigatus* wild-type phytase.

In conclusion, the data presented here show that position 27 is important for determining the specific activity of *A. fumigatus* phytase with phytic acid as substrate. However, in contrast to the narrow substrate specificity observed for *A. terreus* phytase (which has a leucine at the corresponding position), the Q27L and all other mutants at position 27 of *A. fumigatus* phytase maintained the broad substrate specificity characteristic for *A. fumigatus* wild-type phytase. We, therefore, fully achieved our original goal to increase the specific activity of *A. fumigatus* phytase while preserving broad substrate specificity and high activity over a broad pH range. Combined with our "consensus approach" for designing proteins with considerably increased intrinsic thermostability (Lehmann et al., 2000), the present findings should allow development of further improved phytases that are ideally suited for particular applications.

Materials and methods

Homology modeling of A. fumigatus ATCC 13073 and A. terreus CBS (CBS 116.46) phytase

A multiple amino acid sequence alignment of *A. niger* NRRL 3135 phytase, *A. fumigatus* ATCC 13073 phytase, and *A. terreus* CBS phytase (Fig. 1) was calculated with the program PILEUP (Program Manual of the Wisconsin Package, Version 8, Genetics Computer Group, Madison, Wisconsin). Three-dimensional structure models of *A. fumigatus* phytase and *A. terreus* CBS phytase were built by using the structure of *A. niger* NRRL 3135 phytase determined by X-ray crystallography (Kostrewa et al., 1997) as template and exchanging the amino acids of *A. niger* phytase according to the sequence alignment with the respective amino acids of *A. fumigatus* and *A. terreus* CBS phytase. Model construction and energy optimization were performed by using the program Moloc (Gerber & Müller, 1995). C_α positions were kept fixed except for loop regions distant from the active site and for the deletions at positions 1–4, 165, and 444.

DNA constructs and site-directed mutagenesis

Plasmid pUC18-Afum-cDNA, carrying the phytase gene of *A. fumigatus* (Pasamontes et al., 1997a) was used as template to construct the respective mutants. *A. fumigatus* Q27L phytase was obtained by site-directed mutagenesis using the quickchange™ site-directed mutagenesis kit from Stratagene (La Jolla, California) following the manufacturer's protocols. For easy subsequent generation of additional mutants at position 27, a new unique cloning site (AvrII) was introduced upstream of the coding sequence for said amino acid, using the quickchange™ kit. The new plasmid was cut with AvrII and XhoI, and the resulting short phytase gene fragment was replaced by individual linker fragments resulting in the following individual amino acid substitutions at position 27: Q27G, Q27V, Q27N, Q27I, Q27A, and Q27T. The respective sense and antisense polynucleotides used to obtain the individual linkers were as follows:

FumG27-sense:

5′-CTAGGGTACCAGTGCTCCCCTGCGACTTCTCATCTATGGGGC**GGA**TACTCGCCATTCTTTTCGC-3′

FumG27-antisense:

3′-CCATGGTCACGAGGGGACGCTGAAGAGTAGATACCCCG**CCT**ATGAGCGGTAAGAAAAGCGAGCT-5′

For the other amino acid substitutions, the nucleotides in bold were replaced by the following triplets: FumV27-sense, GTG; FumV27-antisense, CAC; FumN27-sense, AAC; FumN27-antisense, TTG; FumI27-sense, ATC; FumI27-antisense, TAG; FumA27-sense, GCG; FumA27-antisense, CGC; FumT27-sense, ACG; FumT27-antisense, TGC. All mutations were confirmed by DNA sequence analysis before subcloning the EcoRV and EcoRI fragment containing the mutated gene into the blunt ended XhoI site and the EcoRI site of the yeast expression vector pYES2 (Invitrogen, San Diego, California).

Plasmid pUC18-Aterrcbs-cDNA carrying the phytase gene of *A. terreus* CBS (van Loon et al., 2000) served as template to construct the *A. terreus* CBS L27Q mutant, using the quickchange™ site-directed mutagenesis kit. Both the wild-type (L27) and the mutated (L27Q) coding sequences of *A. terreus* CBS phytase were isolated with EcoRV and EcoRI and cloned into vector pYES2, as mentioned above.

Expression and purification

Transformation of *Saccharomyces cerevisiae* strain INVSc1 (Invitrogen) with the constructs described above was done according to the manufacturer's instructions, and the recombinant yeast cells harboring the constructs of interest were selected on synthetic dextrose medium plates lacking uracil [SD-(-ura); Sherman et al., 1986]. A single colony was picked, cultivated in 5 mL selection medium [SD-(-ura)] at 30 °C under vigorous shaking (250 rpm) for 3 days, added to 500 ml YPD medium (Sherman et al., 1986) and cultivated for another four days. The cell broth was centrifuged (8,300 × *g*, 15 min, 5 °C) and the supernatant collected and concentrated by ultrafiltration in either Amicon 8400 cells (PM30 membranes; Grace AG, Wallisellen, Switzerland) or ultrafree-15 centrifugal filter devices (Biomax-30K; Millipore, Bedford, Massachusetts).

The concentrate (typically 1.5–5 mL) was desalted in aliquots of 1.5 mL on a Fast Desalting HR 10/10 column (Pharmacia Biotech, Dübendorf, Switzerland), with 10 mM sodium acetate, pH 5.0, serving as elution buffer. The desalted *A. fumigatus* phytase samples were directly loaded onto a 1.7 mL Poros HS/M cation exchange chromatography column (PerSeptive Biosystems, Framingham, Massachusetts). The *A. terreus* CBS L27Q mutant was directly loaded onto a 1.7 mL Poros HQ/M anion exchange chromatogra-

phy column. In both cases, phytase was eluted in pure form by a sodium chloride gradient (0–500 mM).

The data for the *A. fumigatus* and *A. terreus* CBS wild-type enzymes were taken from previous publications (Wyss et al., 1999a, 1999b).

Measurements of enzymatic activity

Standard activity assays were performed at 5 mM substrate concentrations in 200 mM sodium acetate, pH 5.0, and pH-activity profiles with phytic acid determined as previously described (all at 37 °C; Wyss et al., 1999a, 1999b). HPLC analysis of the time course of accumulation of phytic acid degradation intermediates (Fig. 4) was also done as reported previously (Wyss et al., 1999a).

Phosphate liberation kinetics were measured at pH 4.0, 5.0, and 6.0. The purified enzymes were diluted to 0.5 μg/mL in 200 mM sodium acetate buffer with the respective pH. The substrate solution contained 400 μM phytic acid in the respective 200 mM sodium acetate buffer. The reaction was started by mixing equal aliquots of enzyme and substrate solution and stopped after 2, 4, 6, 8, 10, 15, 20, 25, 30, 35, 40, 50, 60, and 90 min of incubation by addition of an equal volume of 15% trichloroacetic acid. Detection of liberated phosphate was carried out as described previously for the standard assay protocol (Wyss et al., 1999b).

Protein determination

Protein concentrations were calculated from the OD at 280 nm, using theoretical absorption values calculated from the known protein sequences with the DNA* software (DNASTAR, Inc., Madison, Wisconsin). An absorption of 1.0 OD at 280 nm corresponds to 0.94 mg/mL of *A. fumigatus* phytase and 0.85 mg/mL of *A. terreus* CBS phytase.

Differential scanning calorimetry

For determination of the unfolding temperature T_m, the proteins purified from *Hansenula polymorpha* culture supernatants were extensively dialyzed against 10 mM sodium acetate, pH 5.0, and concentrated to 50–80 mg/mL. Differential scanning calorimetry was performed as described previously (Brugger et al., 2000). A constant heating rate of 10 °C/min was applied up to 80 °C.

Acknowledgments

Alexandra Kronenberger and Roland Rémy are gratefully acknowledged for technical assistance, and Ulrike Dahlems for construction of the phytase-expressing strains of *Hansenula polymorpha*.

References

Brugger R, Mascarello F, Augem S, van Loon APGM, Wyss M. 2000. Thermal denaturation of fungal phytases and pH 2.5 acid phosphatase studied by differential scanning calorimetry. In: Rasmussen SK, Raboy V, Dalbøge H, Loewus F, eds. *The biochemistry of phytate and phytases*. Dordrecht, The Netherlands: Kluwer Academic Publishers. Forthcoming.

Gerber PR, Müller K. 1995. Moloc molecular modeling software. *J. Comput Aided Mol Design 9*:251–268.

Kostrewa D, Grüninger-Leitch F, D'Arcy A, Broger C, Mitchell D, van Loon APGM. 1997. Crystal structure of phytase from *Aspergillus ficuum* at 2.5 Å resolution. *Nat Struct Biol 4*:185–190.

Lehmann M, Kostrewa D, Wyss M, Brugger R, D'Arcy A, Pasamontes L, van Loon APGM. 2000. From DNA sequence to improved functionality: Using protein sequence comparisons to rapidly design a thermostable consensus phytase. *Protein Eng 13*:49–57.

Lim D, Golovan S, Forsberg CW, Jia Z. 2000. Crystal structures of *Escherichia coli* phytase and its complex with phytate. *Nat Struct Biol 7*:108–113.

Mitchell DB, Vogel K, Weimann BJ, Pasamontes L, van Loon APGM. 1997. The phytase subfamily of histidine acid phosphatases: Isolation of genes for two novel phytases from the fungi *Aspergillus terreus* and *Myceliophthora thermophila*. *Microbiology 143*:245–252.

Pasamontes L, Haiker M, Henriquez-Huecas M, Mitchell DB, van Loon APGM. 1997a. Cloning of the phytases from *Emericella nidulans* and the thermophilic fungus *Talaromyces thermophilus*. *Biochim Biophys Acta 1353*:217–223.

Pasamontes L, Haiker M, Wyss M, Tessier M, van Loon APGM. 1997b. Gene cloning, purification, and characterization of a heat-stable phytase from the fungus *Aspergillus fumigatus*. *Appl Environ Microbiol 63*:1696–1700.

Sherman F, Finck GR, Hicks JB. 1986. *Laboratory course manual for methods in yeast genetics*. Cold Spring Harbor, NY: Cold Spring Harbor Laboratory.

Simões Nunes C, Guggenbuhl P. 1998. Comparative effects of *Aspergillus fumigatus* and *A. niger* phytases on phosphorus and calcium digestibilities and phosphorus faecal excretion in the growing pig. *J Anim Feed Sci 7*: 177–180.

van Etten RL. 1982. Human prostatic acid phosphatase: A histidine phosphatase. *Ann NY Acad Sci 390*:27–51.

van Loon APGM, Simões-Nunes C, Wyss M, Tomschy A, Vogel K, Pasamontes L. 2000. A heat-resistant phytase of *Aspergillus fumigatus* with superior performance in animal experiments. Phytase optimization and natural variability. In: Rasmussen SK, Raboy V, Dalbøge H, Loewus F, eds. *The biochemistry of phytate and phytases*. Dordrecht, The Netherlands: Kluwer Academic Publishers. Forthcoming.

Wodzinski RJ, Ullah AHJ. 1996. Phytase. *Adv Appl Microbiol 42*:263–302.

Wyss M, Brugger R, Kronenberger A, Rémy R, Fimbel R, Oesterhelt G, Lehmann M, van Loon APGM. 1999a. Biochemical characterization of fungal phytases (*myo*-inositol hexakisphosphate phosphohydrolases): Catalytic properties. *Appl Environ Microbiol 65*:367–373.

Wyss M, Pasamontes L, Friedlein A, Rémy R, Tessier M, Kronenberger A, Middendorf A, Lehmann M, Schnoebelen L, Röthlisberger U, Kusznir E, et al. 1999b. Biophysical characterization of fungal phytases (*myo*-inositol hexakisphosphate phosphohydrolases): Molecular size, glycosylation pattern and engineering of proteolytic resistance. *Appl Environ Microbiol 65*:359–366.

Wyss M, Pasamontes L, Rémy R, Kohler J, Kusznir E, Gadient M, Müller F, van Loon APGM. 1998. Comparison of the thermostability properties of three acid phosphatases from molds: *Aspergillus fumigatus* phytase, *A. niger* phytase, and *A. niger* pH 2.5 acid phosphatase. *Appl Environ Microbiol 64*:4446–4451.